Organic & Biomolecular Chemistry

PAPER

View Article Online
View Journal | View Issue

Cite this: *Org. Biomol. Chem.*, 2016, **14**, 8707

Tetra-porphyrin molecular tweezers: two binding sites linked *via* a polycyclic scaffold and rotating phenyl diimide core†

R. B. Murphy,[a] R. E. Norman,[a] J. M. White,[b] M. V. Perkins[a] and M. R. Johnston*[a]

Received 26th July 2016,
Accepted 18th August 2016

DOI: 10.1039/c6ob01588c

www.rsc.org/obc

The synthesis of a tetra-porphyrin molecular tweezer with two binding sites is described. The bis-porphyrin binding sites are aligned by a polycyclic scaffold and linked *via* a freely rotating phenyl diimide core. Synthesis was achieved using a divergent approach employing a novel coupling method for linking two polycyclic units to construct the core, with a copper(II)-mediated phenyl boronic acid coupling found to extend to our polycyclic imide derivative. We expect this chemistry to be a powerful tool in accessing functional polycyclic supramolecular architectures in applications where north/south reactivity and/or directional interactions between modules are important. Porphyrin receptor functionalisation was undertaken last, by a four-fold ACE coupling reaction on the tetra-epoxide derivative of the core.

Introduction

Molecular tweezers containing two ligand binding sites, where these are remote but interdependent, can benefit from co-operativity during complexation, to positively or negatively influence ligand binding. Several examples of cooperativity in molecular tweezers appear in the literature, from early architectures such as Rebek's 2,2′-bipyridine/crown ether system,[1–3] to more recent bis-porphyrin systems with either crown ether,[4,5] pyridyl,[6] or biindole[7] effector sites. Molecular-based stimuli can also be used to effect changes to guest binding in molecular tweezers. For example, a water-soluble polymer-tethered tweezer has shown progress towards the development of controlled drug release devices, using a proton-activated (pH) switching unit to change the conformation of bis-naphthalene receptors and release a substrate.[8] Cooperativity has even been shown to arise from electronic rather than steric effects,[9,10] by using the direction of charge transfer (CT) between a porphyrin host and an appropriate guest (CT donor or acceptor).

We have previously described the synthesis and binding characteristics of single binding site tweezer system **1**[11] (Fig. 1), in which the bis-metalloporphyrin receptor offers strong intramolecular complexation with the diamino ligand 1,4-diazabicyclo[2.2.2]octane (DABCO).

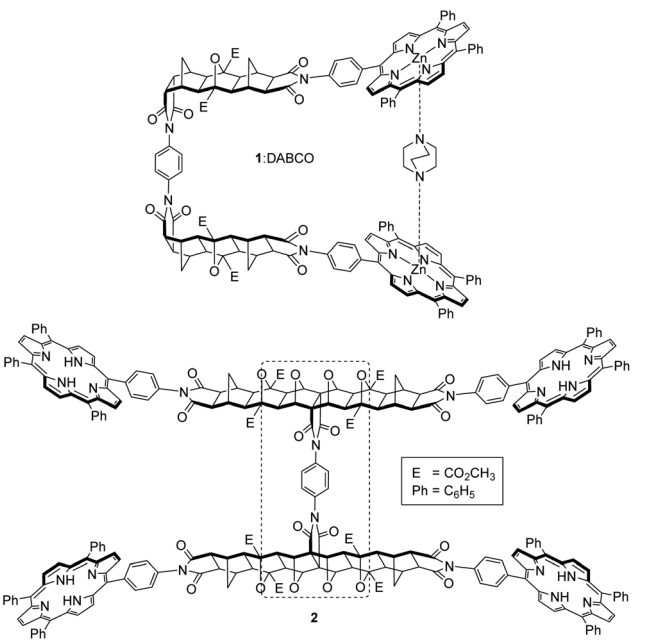

Fig. 1 Previously described model tweezer system **1**[11] (shown as complex with DABCO), and the expanded tetra-porphyrin molecular tweezer **2** with two bis-porphyrin binding sites linked *via* a bridged polycyclic scaffold and freely rotating phenyl diimide core (dotted line).

[a]*Flinders Centre for NanoScale Science and Technology, School of Chemical and Physical Sciences, Flinders University, Bedford Park, Adelaide, Australia. E-mail: martin.johnston@flinders.edu.au*
[b]*School of Chemistry, The University of Melbourne, Melbourne, Australia*

†Electronic supplementary information (ESI) available: NMR, X-ray crystallographic data, and UV-Vis and HRMS for porphyrin compounds. CCDC 1486427–1486430. For ESI and crystallographic data in CIF or other electronic format see DOI: 10.1039/c6ob01588c

Polycyclic frameworks, based on norbornyl derivatives, provide several distinct advantages when incorporated into molecular tweezers; namely excellent control of the direction of both lateral and vertical extension and well defined positioning of pendant moieties. These structures are highly synthetically variable using chemistry developed extensively by the research groups of Warrener and Butler[12–16] and Paddon-Row,[17–20] and is very much modular, enabling the synthesis of supramolecular architectures with customisable dimensions. More recent examples include those by the groups of Johnston,[21,22] Pfeffer,[23,24] and Margetić.[25–27] Molecular modelling by Warrener[28,29] and Johnston,[30] and experimental evidence by Margetić[26] has shown that the inclusion of certain modules provides either linearity or curvature to the polycyclic scaffold. Importantly, a number of studies by several research groups has identified that polycyclic backbones are characterised by a higher degree of rigidity when only consisting of fused bridged polycyclic rings, with non-bridged cyclohexane(ene) rings and fused aromatic rings increasing flexibility.[19,20,31–37] However, caution must be exercised, as small degrees of flexibility within rigid modular sections can be amplified across the complete scaffold.[38]

Our original bis-porphyrin tweezer model architecture **1** has now been expanded to tetra-porphyrin system **2** with two homotropic binding sites (Fig. 1). We reasoned that with the inclusion of a largely rigid polycyclic backbone, the inter-porphyrin distance from the binding of one guest may be able to be transferred to a second remote site with interannular cooperativity. This type of cooperativity arises in systems when there is interplay between two or more intramolecular binding interactions.[39] The two polycyclic backbones would be connected *via* a centrally located phenyl diimide structural unit, which would be fundamental in conferring the rotational degrees of freedom required by the host to facilitate interannular cooperativity between the two remote but interdependent binding sites. Furthermore, rotation about the porphyrin-polycyclic backbone bonds would allow for further cavity adjustment as required by different sized guests.

Results and discussion

Two overall approaches to synthesising **2** were considered; convergent and divergent (Fig. 2). The convergent approach, whereby *p*-phenylenediamine is used to link two bis-porphyrin alicyclic systems *via* their anhydride (Fig. 2a), is synthetically preferable as this route provides increased structural control; functionalisation of each half with porphyrin receptors involves two points of reactivity.

On the contrary, a divergent approach was envisaged in which two alicyclic systems were already linked to create a central core, to which porphyrin receptors could be subsequently attached (Fig. 2b). This avenue provides less structural control, as building out from the core would involve four simultaneous points of reactivity during receptor functionalisation.

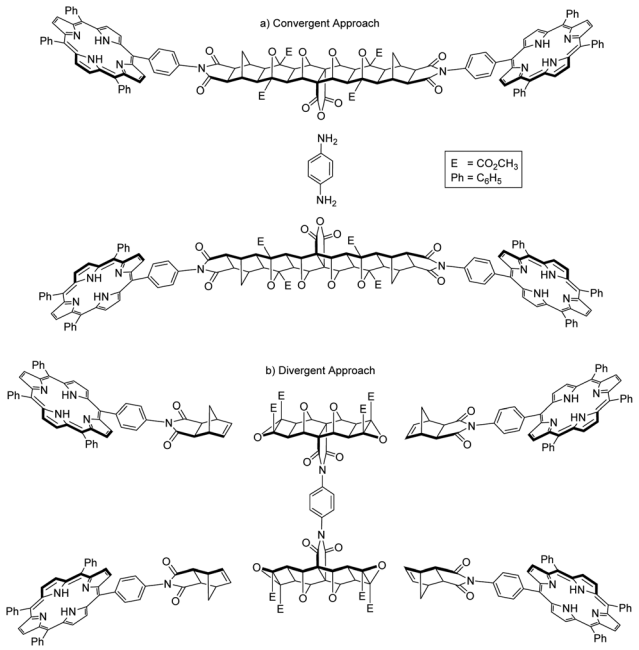

Fig. 2 Schematic representations of convergent and divergent synthetic approaches to the synthesis of tetra-porphyrin tweezer **2**.

Convergent approach towards 2

Initial attempts focused on the convergent approach since this was envisaged to allow the highest degree of control over the final system synthesised. This began with the application of Mitsudo conditions[40,41] to anhydride functionalised bis-oxa block **3** (Fig. 3), and which afforded the bis-(cyclobutene methyl ester) adduct **4**[42] in excellent yield. This was subsequently epoxidised in the normal manner,[14,16] giving bis-epoxide **5** in good yield. Microwave-accelerated ACE reaction[43] with mono-porphyrin receptor **6**[11] successfully generated the bis-porphyrin anhydride **7**. The identity of **7** was confirmed by

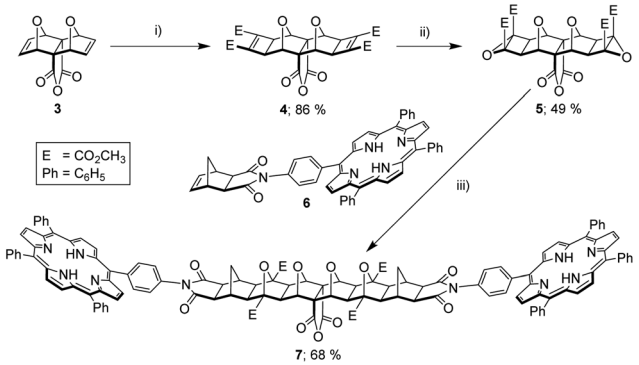

Fig. 3 Convergent synthetic approach *via* bis-porphyrin anhydride **7**. (i) DMAD (2 eq.), 5 mol% $[RuH_2(CO)(PPh_3)_3]$, toluene, 80 °C, N_2 atmosphere, 4 days, 86%; (ii) anhydrous 3.3 M *t*BuOOH in toluene (2.5 eq.), dry CH_2Cl_2, 0 °C, N_2 atmosphere, 10 min, *t*BuOK (1 eq.), r.t., 3.5 h, 49%; (iii) *exo*-porphyrin receptor **6** (2 eq.), dry THF, microwave 80–220 W, 14–20 bar, 170 °C, 2 h, 68%.

HRMS (S5,† calcd $[M + 2H]^{2+}$ 1050.3421, found 1050.3432), as poor solubility, presumably due to aggregation, in many organic solvents prohibited characterisation by NMR.

As the bis-porphyrin anhydride **7** displayed poor solubility in common organic solvents, the Mitsudo anhydride **4** was employed as a soluble model compound in an attempt to ascertain whether the convergent synthesis could be completed as represented in Fig. 2a. **4** was frustratingly unable to be successfully reacted with aromatic amines under a variety of conditions. In summary, these problems stem from the *exo*-bis-oxa-polycyclic moiety, which unfortunately exhibits a combination of thermal instability prior to lateral functionalisation (retro-Diels–Alder),[12,15,38,44,45] and poor anhydride reactivity *via* conventional condensation with aromatic amines,[38,44] particularly following lateral functionalisation.[45] It has been suggested by others that the anhydride is shielded by *endo*-hydrogen atoms at the ring junctions in laterally functionalised derivatives.[45] Thus even if a highly soluble derivative of bis-porphyrin anhydride **7** could be synthesised, condensation with *p*-phenylenediamine would not be a viable convergent pathway to the tetra-porphyrin tweezer **2**. Hence, our hand was forced to pursue a divergent approach.

Divergent approach towards 2

The divergent approach comprised the synthesis of the phenyl diimide core and subsequent attachment of the porphyrin moieties. Retrosynthetic analysis of the phenyl diimide core (dotted line, Fig. 1) was undertaken and is shown in Fig. 4.

The *endo*-functionality of the polycyclic module (R^1 in Fig. 4) can be the dicarboxylic acid,[46,47] diacid chloride,[38,48] anhydride,[49] or imide[18,50–53] derivative. The 1,4-substituted phenyl core then needs to possess a functionality (R^2 in Fig. 4) suitable for reaction with the aforementioned functional groups. For example, literature precedent exists for the condensation of the diacid chloride derivative **8** with aniline derivatives (Fig. 5).[38,44] Alternatively, while the anhydride **3** does not ordinarily react with aniline derivatives, reaction has been reported for non-laterally functionalised anhydride **3** when the aniline derivative is deprotonated by strong base such as *n*-BuLi.[45]

We chose a combination of these two conditions and utilised the reactivity of acid chloride **8** with the increased nucleophilicity[54] of the *p*-phenylenediamine mono-anion following deprotonation by a strong base, in this case LiHMDS (Fig. 5). This afforded a significant improvement in the reaction time over the aforementioned literature methods, with instant precipitation of the intermediate amic acid from the reaction mixture. Subsequent carbodiimide-mediated ring closing of the amic acid to the imide yielded the tweezer core structure **9**, with identical NMR spectra (see S6†) to that reported.[44]

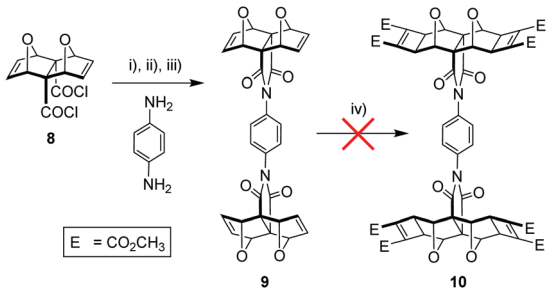

Fig. 5 (i) *p*-phenylenediamine, THF, N_2 atmosphere, r.t., slow addition of <1 eq. LiHMDS, stirring 30 min, (ii) diacid chloride (2 eq.), N_2 atmosphere, r.t., 1 h, (iii) HOBt/DCC/Et_3N, dry THF, N_2 atmosphere, r.t., 3 days; (iv) DMAD (8 eq.), 20 mol% $[RuH_2(CO)(PPh_3)_3]$, toluene, 50 °C, N_2 atmosphere, 3 days, no reaction.

Conveniently, we obtained a crystal of **9** from DMSO solution suitable for X-ray crystallographic analysis. Solving of the structure revealed the structure shown in Fig. 6. The structure of **9** has a crystallographic centre of inversion and is co-crystallised with two molecules of DMSO which occupy channels extending along the *a*-direction in the crystal. Additional information on the crystal structure of compound **9** can be found in the ESI (see S8†).

The next step towards the necessary tetra-functional phenyl diimide core **10** was a Mitsudo [2 + 2] cycloaddition reaction using DMAD and a ruthenium catalyst. Unfortunately, core unit **9** was found to be unreactive to Mitsudo conditions (Fig. 5), a problem we had encountered previously during the corresponding linker synthesis for tweezer **1**.[55] Unfortunately, the retro-Diels–Alder potential of **9** limited the harshness of the conditions that were able to be employed in forcing the Mitsudo reaction, and we were unable to achieve any success in this regard. There are only a few norbornyl based substrates

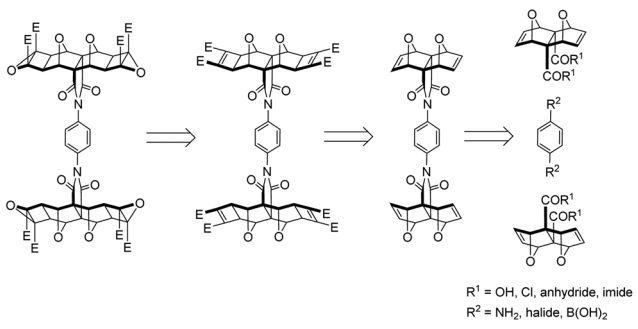

Fig. 4 Retrosynthetic analysis of the phenyl diimide core.

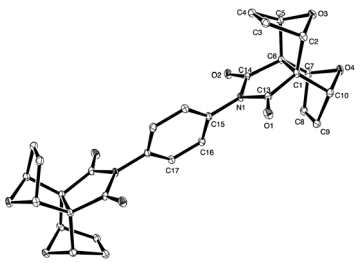

Fig. 6 X-ray crystal structure of the centrosymmetric phenyl diimide core **9**. The DMSO molecules have been omitted for clarity, H atoms are not shown.

identified in the literature that do not undergo the Mitsudo reaction,[56] with no clear trends evident with our compounds, or similar compounds in the literature that allow this result to be rationalised. Further investigations are currently underway in our laboratory in an attempt to rationalise this lack of reactivity of this as well as several other substrates.

It became evident from both our own work and the work of others[38,44,45] that the known syntheses currently employed for polycyclic substrates would be unsuitable to generate the tetra-functional core **10** (Fig. 5) required for the tetra-porphyrin tweezer **2**. Faced with the competing triad of thermal instability of **3** and **9**, poor anhydride reactivity of laterally functionalised **4** with aromatic amines, and the inability of the core unit **9** to undergo the Mitsudo reaction, we required a substrate to circumvent each of these complications. The imide **13** (Fig. 7) alleviated all of these issues; (i) reactivity in the southern direction is moved from the carbonyl to the imide nitrogen avoiding the steric protecting effects of the adjacent *endo*-hydrogen atoms on anhydride reactivity, and (ii) pre-installed cyclobutene rings (Mitsudo reaction) both prevent thermal degradation and commence lateral functionalisation.

Fortunately, there was literature precedent for the non-Mitsudo imide **12**,[18,50] in two steps from anhydride **3**. This method uses *p*-methoxybenzylamine (PMB) as a nitrogen source, with the intermediate PMB-protected derivative **11** cleaved to yield the free imide **12** (Fig. 7). We prepared **12** using these literature methods and then applied Mitsudo conditions to afford the imide **13**.

We were fortunate to obtain X-ray quality crystals for all three compounds in this synthetic series to confidently assign the structures of imides **11**, **12** and **13** (Fig. 8). The structures of all three imide block derivatives contain two 7-oxabicycloheptane motifs with a 6-membered ring A and 5-membered ring B approximately perpendicular. The fusion of these rings adopt an *envelope* conformation in compounds **11–13** with an O atom as the flap. The skeletal framework of these molecules is a strained system (bridgehead O atom bond angles of 96–97° for **11** and **12**, and 98° for **13**, refer to S15†).

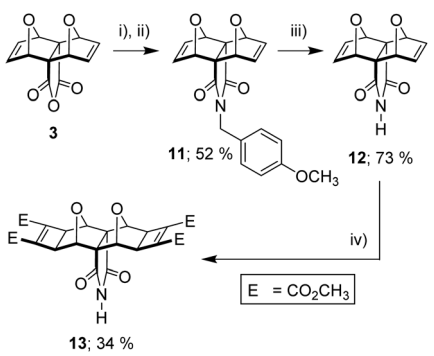

Fig. 7 (i) *p*-methoxybenzylamine (2 eq.), deacidified $CHCl_3$, 50 °C, N_2 atmosphere, overnight; (ii) $NaOAc/Ac_2O$, 50 °C, N_2 atmosphere, overnight, 52%; (iii) 9 : 1 CH_3CN/H_2O, ammonium cerium(IV) nitrate (3.3 eq., 2 h; 2.3 eq. 90 min + 1 eq. 30 min), 40 °C, 73%; (iv) DMAD (4 eq.), 36 mol% $[RuH_2(CO)(PPh_3)_3]$, dry DMF, 60 °C, N_2 atmosphere, 24 h, 34%.

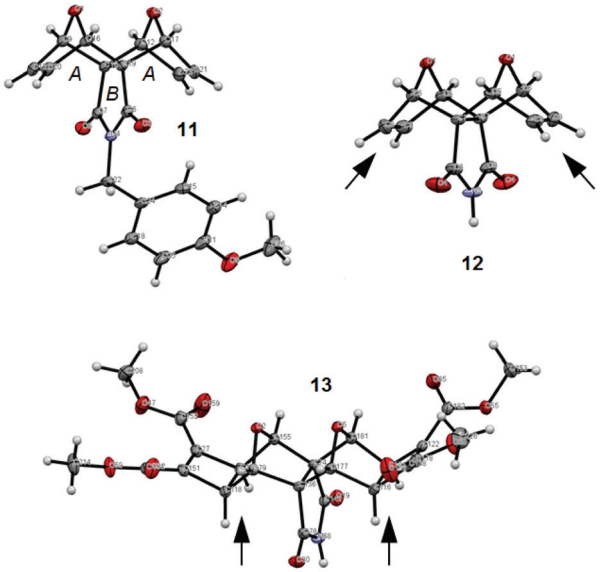

Fig. 8 X-ray crystal structures of the imide series **11**, **12** and **13**. The arrows highlight the change in the position of the hydrogen atoms at the ring junctions following addition of the cyclobutene diester ring.

The non-Mitsudo imide **12** is centrosymmetric and solved as the asymmetric unit with SHELX-97 in a monoclinic unit cell (space group *P*21/*c*). In structure **12**, the crystal packing features intermolecular N2–H2···O1 hydrogen bonding features (see S15†); whereas the PMB protected imide **11** does not exhibit such interactions. Within the crystal lattice of the imide **13** there exists hydrogen bonding contacts between the *envelope* flap oxygen atoms (O18/O5/O3 and O15/O2/O11) with a molecule of water (see S15†). The imide nitrogen atoms (N36, N48, N68) interact with the same water molecules, as do the C=O oxygen atoms from the methyl esters (O203, O87). This creates a pseudo coordination center about each H_2O molecule. There are no interactions observed with the CH_3CN molecules. Additional information on the crystal structures of compounds **11–13** can be found in the ESI (see S15†).

Furthermore, the X-ray crystal structures **12** and **13** reveal significant differences in the position of the hydrogen atoms at the ring junctions as the hybridisation of the carbon atom changes from sp^2 to sp^3 (marked with arrows in Fig. 8). This could support the notion previously reported by others that the anhydride is shielded[45] in laterally functionalised derivatives.

The next step in the divergent approach towards **2** was the coupling of two units of imide **13** together through the imide nitrogen atom. On review of the literature, two candidates for coupling nitrogen-containing molecules with aryl species were identified, neither of which appeared to have been demonstrated on norbornyl imides to our knowledge.

Imide–aryl halide Cu(0) coupling. Initially, a microwave-assisted copper(0)-mediated aryl halide–imide coupling was explored, as reported for phthalimide with a mono-halo aryl species.[57] We applied these reaction conditions to imide **13**

and model substrate iodobenzene (Fig. 9). This was found to successfully yield **14a** by using excess iodobenzene (as the solvent) at 150 °C utilising several cycles through the microwave. These reaction conditions were then applied to the synthesis of diimide **10** using 1,4-diiodobenzene rather than iodobenzene. Unfortunately, the synthesis of the phenyl diimide **10** was more challenging and no appreciable amounts were detected in the reaction mixture. The solid nature of the 1,4-diiodobenzene required solvent for adequate mixing with **13**, resulting in dilute reactant concentrations for stoichiometric quantities of aryl halide. This technique was further complicated by reaction vessels being prone to fracture from either spot heating of elemental copper by the microwave reactor, or from rapid temperature fluctuations and pressurisation in the case of a solventless melt.

A small quantity of the asymmetric phenyl 1-imide-4-iodo adduct **14b** was generated by using excess 1,4-diiodobenzene in solvent and subjecting to microwave irradiation in several cycles over approximately 12 hours. However, the inefficiency associated with forming precursor **14b**, along with the second coupling of **13** with **14b** (not attempted) which would be required to generate diimide **10** led us to explore an alternative imide coupling procedure.

Imide–boronic acid Cu(II) coupling. An alternative candidate involved the coupling of N–H with aryl boronic acids. This has been previously reported for aryl mono-boronic acid derivatives with nitrogen-containing compounds[58,59] such as imidazole, amines, amides, sulfonamides, and imides phthalimide and succinimide, under simple Cu(II) salt catalysis. The reaction proceeds in protic solvent without additives such as bases or ligands.[58,59] We found substitution of these nitrogen-containing compounds with our polycyclic imide **13**, using phenyl boronic acid under the conditions described,[58,59] gave **14a** (based on ^{1}H NMR spectra).

Given the success of this coupling reaction, we employed 1,4-phenyl diboronic acid and polycyclic imide **13**, in a 1 : 2 stoichiometric quantity, to produce phenyl diimide **10** (Fig. 10). The identity of **10** was confirmed by HRMS (calcd $[M + Na]^+$ 1127.2182, found 1127.2166), while the ^{1}H and

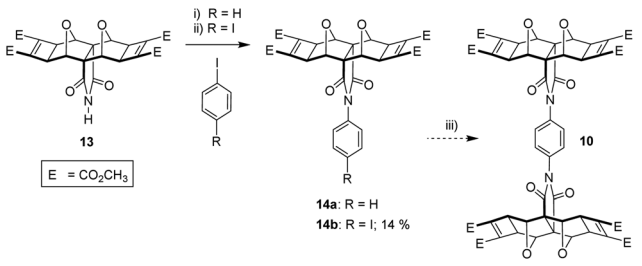

Fig. 9 (i) 1-Iodobenzene (excess, as solvent), freshly precipitated Cu(0) (5 eq.), 4 × 10 minute microwave cycles (300 W, high stirring, air cooling, 150 °C); (ii) Initially 1,4-diodobenzene (8 eq.), freshly precipitated Cu(0) (8 eq.), EtOAc (1 mL), microwave settings as for step (i), 120–150 °C, 1 h. Then further addition of Cu(0) (8 eq.), microwave, 120–150 °C, 1.5 h. Addition of toluene (1 mL), microwave, 150 °C, 1 h + 8.5 h. 14% of **14b**; (iii) **14b**, **13** (1 eq.), not attempted.

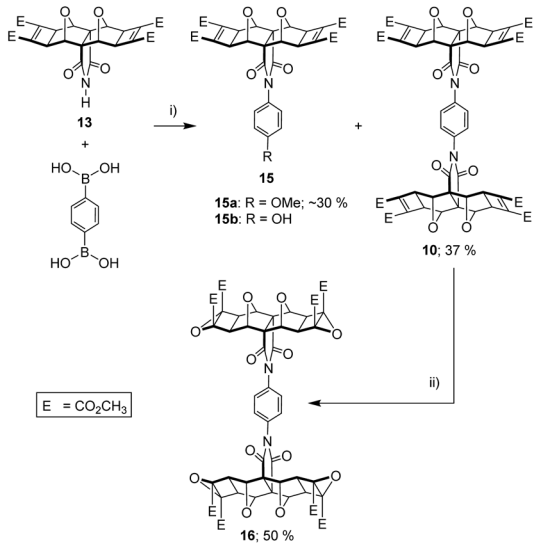

Fig. 10 (i) benzene-1,4-diboronic acid, copper(II) acetate (5 mol% per boronic acid), MeOH or 9 : 1 THF/H_2O, reflux, air bubbler, 18 h, ~30% **15a** + 37% **10**; (ii) anhydrous 3.3 M *t*BuOOH in toluene (5 eq.), dry CH_2Cl_2, 0 °C, N_2 atmosphere, 10 min, *t*BuOK (2 eq.), r.t., 3.5 h, 50%.

^{13}C NMR spectra (see S18 and S19†) both showed the expected number of resonances. A singlet in the ^{1}H NMR at 7.38 ppm was assigned to the phenyl core and suggests that the rotation of both phenyl–imide bonds is rapid on the NMR timescale.

The optimum Cu(II) catalyst loading was found to be less than 5%, at which the reaction yielded approximately equal quantities of unreacted starting material imide **13**, desired product **10**, but also an unexpected side product **15** (Fig. 10). This side product was identified as **15a** or **15b** depending on the solvent used for the reaction (see next paragraph). These products indicate a competitive reaction between boronic acid, imide, and solvent. At greater than 5% catalyst loadings, side product **15** became the major product. These side products were not reported in the original methods,[58,59] which only use aryl mono-boronic acid derivatives, and this led us to briefly explore the effect of solvent on the coupling reaction.

As reported in the original methods, we also found that no coupling was obtained in aprotic solvents such as THF, but that successful coupling could be achieved protic solvents such as MeOH, or mixed aprotic/protic solvents such as THF/H_2O.[58,59] In our case, THF/H_2O (9 : 1) yielded not only the phenyl diimide **10**, but side product with hydroxy substitution **15b**. When the solvent was MeOH, the side product was methoxy substituted **15a**.

Even with this side reaction, a sufficient quantity of the tetra-functional phenyl diimide core **10** was obtained to allow further reactions to be carried out. Thus **10** was subsequently subjected to a four-fold nucleophilic epoxidation at the electron deficient alkene, which gave decent yields of tetra-epoxide **16** (Fig. 10). The identity of tetra-epoxide **16** was confirmed by using HRMS (calcd $[M + Na]^+$ 1191.1978, found 1191.1984, 1191.2006). The successful incorporation of the epoxide

functionality set the stage for the ACE coupling to attach the porphyrin moieties.

Tetra-porphyrin tweezer

The tetra-epoxide core **16** was appended with *exo*-porphyrin receptors **6**[11] *via* the alkene plus cyclobutane epoxide (ACE) reaction (Fig. 11), accelerated by the use of microwave irradiation.[43] Although ACE chemistry has been well established for polycyclic scaffolds for some time, there appears to be no examples of tetra-functional substrates undergoing four simultaneous ACE reactions. The tetra-porphyrin two binding site tweezer **2** was found to be the major product of the reaction (by ^{1}H NMR of the crude reaction mixture), however, the high degree of purity required for host–guest experiments resulted in significant loss of product from column chromatography and repeated recrystallisations to remove traces of the other porphyrin stoichiometries. The identity of the freebase tweezer **2** was confirmed by using HRMS (see S25,† calcd $[M + 4H]^{4+}$ 1068.3540, found 1068.3566, plus $[M + 3H]^{3+}$ and $[M + 2H]^{2+}$).

The ^{1}H NMR spectra reflected the symmetry of the tetra-porphyrin tweezer **2**, arising from free rotation about the phenyl diimide core and porphyrin receptors. Several features characteristic of ACE-coupled reaction products could be observed, including a small downfield shift for the methyl ester resonance,[43] along with the disappearance of the norbornene proton resonance from the *exo*-receptor **6** at 6.45 ppm. The resonance at 90 ppm in the ^{13}C NMR spectrum (not shown) is observed in similar polycyclic systems,[34] and is assigned to the carbon bridgehead atoms in the newly formed oxanorbornane.[34]

In the ^{1}H NMR spectrum (see S24†), seven polycyclic resonances can be observed as expected (excluding the methyl ester); five singlets and two doublets. Of the five singlets, two arise from the central 7-oxanorbornane component, labelled 1–2, Fig. 11), while the remaining three signals arise from the *exo*-component (labelled 3–5, Fig. 11). The doublets, which occur at chemical shifts of 1.27 and 2.62 ppm, correspond to the methylene bridge protons H_a/H_b (Fig. 11), which appear at different chemical shifts due to the influence of the 7-oxanorbornane in these linear systems.[25,26,30]

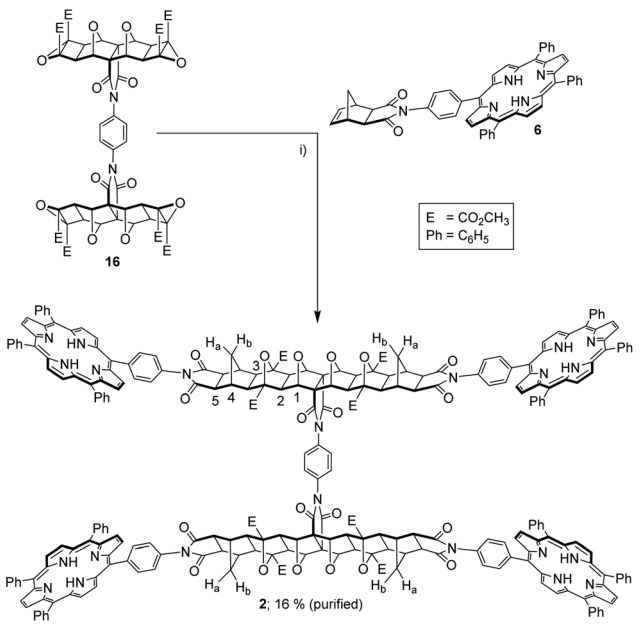

Fig. 11 (i) *exo*-Porphyrin receptor **6** (4 eq.), dry THF, microwave 80–220 W, 14–20 bar, 170 °C, 2 h, 16% after purification.

Table 1 Summary of UV-Vis data in chloroform (10^{-6}–10^{-7} M)

Species	Freebase mono-porphyrin receptor **6**[11]	Freebase bis-porphyrin tweezer **1**[11]	Freebase tetra-porphyrin tweezer **2**
λ_{max} (nm)	418.9	419.0	419.0
Width (nm)[a]	11.8	12.5	12.1

[a] Peak band width measured at half height.

There is some evidence of facial differentiation within the porphyrin macrocycles in the ^{1}H NMR spectrum of the freebase tetra-porphyrin tweezer **2** (see S24†). While the β-pyrrole resonance appears as a singlet, there is slight splitting/desymmetrisation within some of the *meso*-phenyl resonances, and the linking *meso*-phenyl resonances are somewhat broad (see S24†). This facial differentiation indicates there is some amount of either intramolecular interaction of opposing porphyrins or intermolecular aggregation at NMR concentrations (10^{-3}–10^{-4} M).

The various porphyrin containing molecules were also examined using UV-Vis spectroscopy. Table 1 summarises the main spectral features of the freebase derivatives of the tetra-porphyrin tweezer **2** (see S26†), bis-porphyrin tweezer **1**,[11] and mono-porphyrin receptor **6**. The Soret peak band width of 12.1 nm for tetra-porphyrin tweezer **2** is barely broadened compared to the value for mono-porphyrin receptor **6** (11.8 nm), indicating that exciton coupling interactions between the porphyrins in the tetra-porphyrin tweezer **2** are largely absent at UV-Vis concentrations (10^{-6}–10^{-7} M). This suggests either the porphyrin units are able to undergo rotation either about the single bond between the imide and/or porphyrin moiety, and/or the two polycyclic arms can undergo rotation about the central phenyl diimide core.

Molecular modelling

It was envisaged that an unsubstituted central phenyl core would confer the rotational ability required by the polycyclic scaffold to facilitate interannular cooperativity between the two remote binding sites. A significant number of computational and experimental works exploring bond rotation in *N*-phenyl imide derivatives have been reported.[60–76] In summary, the energy barrier to rotation increases as the size of the *ortho*-phenyl substituent increases due to steric repulsion between the substituent and the oxygen atom of the imide.[60,64,65] Additionally, the angle between the aryl and imide rings increases towards perpendicular with increasing size of the *ortho*-substituent on the phenyl ring, to minimise steric repul-

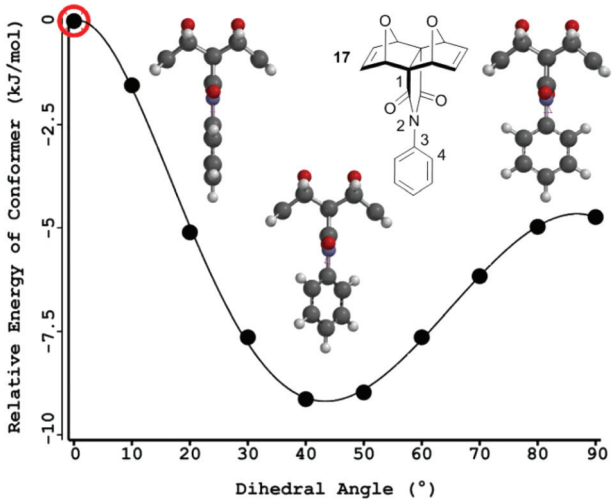

Fig. 12 Rotational energy profile and barrier to rotation about the imide–phenyl single bond in a model of the linker, compound **17** (energy profile Hartree–Fock 6-31G*, energy of each conformation recalculated Density Functional B3LYP/6-31G*).

sion between the substituent and the oxygen atom of the imide.[60–62,64] This competes with the resonance delocalisation and conjugation favoured in the planar conformation[77]‡. Free rotation is reported for unsubstituted *N*-phenyl imide derivatives,[66,67] with rotation becoming restricted for *ortho*-substituents other than hydrogen,[66–76] while *meta*- and *para*-phenyl substitution does not affect rotation in these systems.[67]

To gain an increased understanding of the barrier to rotation about the imide–phenyl bond at the core of tetra-porphyrin tweezer **2**, a rotational energy profile was calculated§ for a simplified model of the linker, compound **17**¶ (N_2–C_3, Fig. 12). The relative energy difference between the global maximum and minimum is approximately 9 kJ mol^{-1} (2.15 kcal mol^{-1}) and supports the notion of free rotation in this system at room temperature, from thermal energy available from the surroundings.[65] Not surprisingly, the highest energy conformer occurs at a dihedral angle of 0°, when the phenyl ring proton atoms and imide carbonyl oxygen atoms are in the same plane and interacting sterically. The lowest energy conformation occurs at a dihedral angle of approximately 45°, while a local maximum occurs at approximately 90°.

Molecular modelling has been previously used to calculate the ground state optimised geometry in a polycyclic *N*-phenyl imide system.[17,78] In this study, the global energy minimum corresponded to a phenyl–imide angle of 70–71° (RHF/3-21G,[78] HF3-21G[17]), and was 5.65 kJ (1.35 kcal) more stable than the case where the phenyl ring was constrained to the plane of the imide.[78] While the phenyl–imide angle for the global energy minimum is different depending on the computational method employed (rotational energy profile in our work, and the ground state optimised geometry in the literature[17,78]), both calculations confer that the highest energy state occurs when the phenyl ring is in the plane of the imide, where the hydrogen and oxygen atoms are sterically interacting.

In the absence of X-ray crystallographic data, molecular modelling[79] was undertaken to provide information on the equilibrium geometry of the two binding site tweezer **2**. Fig. 13 shows the equilibrium geometry (semi-empirical, AM1) of the zinc(II) metallated adduct of tetra-porphyrin tweezer **2** without guest, and indicates that the polycyclic scaffolds do not necessarily adopt a parallel alignment, as per the idealised structures shown in the reaction schemes, with the two polycyclic arms rotated with respect to each other around the central phenyl diimide group. The phenyl–imide angle from this model of **2** was calculated to be 43° or 21° (depending on whether measured from either the top or bottom half of the model), and is within the trough of the rotational energy profile shown earlier for compound **17** in Fig. 12.

In addition, the idealised parallel arrangement of the porphyrin units has been replaced by a skewed interporphyrin geometry as a result of rotation about the imide–phenyl–porphyrin bond. Rotation of porphyrins about unsubstituted *meso*-phenyl rings with respect to the porphyrin β-pyrrole region is well known.[80–82] Thus the freely rotating porphyrin receptors provides the system with the ability to cofacially

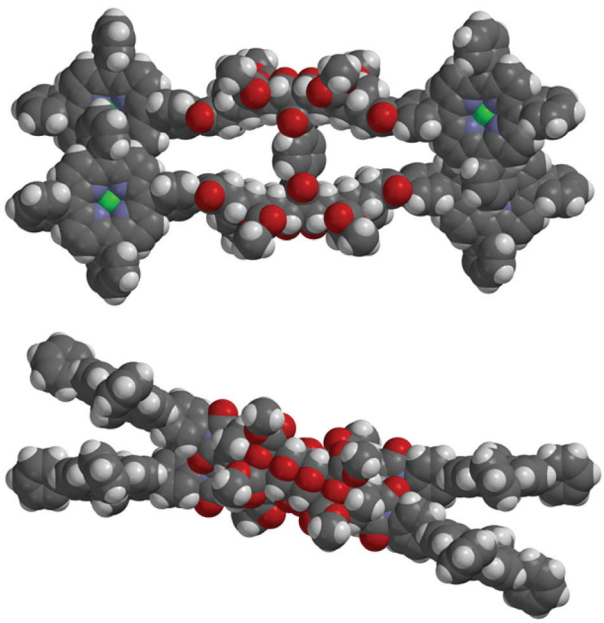

Fig. 13 Molecular modelling of the zinc(II) metallated adduct of the two binding site tetra-porphyrin tweezer **2** in the absence of guest (side-on and top-down) (semi-empirical, AM1).

‡Ref. 77 refers to anilide derivatives rather than imides, however, the principle of balancing steric and electronic factors is the same here.

§Refer to the molecular modelling paragraph in the Experimental section for computational information regarding this calculation.

¶This simplified model of the linker does not account for possible additional steric crowding on the underside of the polycyclic arms when additional polycycles are fused to the linker, or the possible electronic effect on rotation due to the second *para*-imide (as in compound **10**). The potential stabilising π–π interactions between the opposing bis-porphyrins are also not accounted for by model compound **17**.

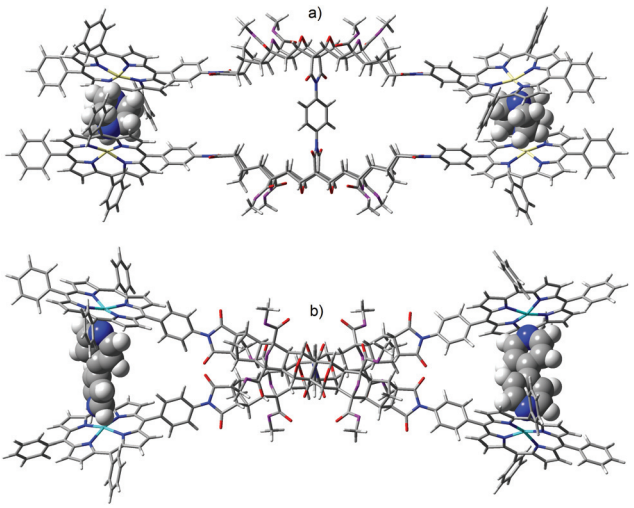

Fig. 14 Molecular modelling of the zinc(II) metallated adduct of the two binding site tetra-porphyrin tweezer **2** in the presence of diamino ligands; (a) **2**:$(DABCO)_2$ (side-on), (b) **2**:$(bipy)_2$ (top-down) (semi-empirical, AM1).Image rendered in GaussView.‖

align the bis-porphyrins after undergoing defined changes to interporphyrin distance upon guest binding as the polycyclic scaffold is rotated through the central core.

Another structural feature not accounted for by the reaction scheme structures is the high degree of curvature in polycyclic scaffolds with 7-oxanorbornane modules.[28,29] This is clearly observable in the molecular models in Fig. 13, and is a crucial design feature in our tweezer which enables the bis-porphyrin binding sites to be coplanar in each half[30] and cofacial between the two halves, if an idealised conformation is adopted in the presence of a guest.

Fig. 14 shows the equilibrium geometry of the zinc(II) metallated adduct of tetra-porphyrin tweezer **2** with diamino ligand; for (a) DABCO and (b) 4,4′-bipy. The system appears able to accommodate diamino ligands of different lengths (N–N distance for DABCO is 2.6 Å, 7.2 Å for 4,4′-bipy, semi-empirical AM1) as eluded to previously, by rotating both the rigid polycyclic arms (*via* the phenyl diimide core) and the porphyrin receptors, to adjust the interporphyrin distance as required. For example, the polycyclic arms are rotated further with respect to each other for bipy than for DABCO, due to the difference in ligand length. With respect to each guest, approximately equal interporphyrin distance was observed at both binding sites. Neither the DABCO nor bipy complexed structures appear to be significantly strained, and overlay of the polycyclic arms for molecular models with and without guest (not shown) revealed only minimal distortion, providing further evidence that the polycyclic arms are largely rigid. The experimental host–guest complexation of the zinc(II) metallated adduct of tetra-porphyrin tweezer **2** with diamino ligands, and analysis of interannular cooperativity will be described in a future publication.

‖R. Dennington, T. Keith and J. Millam, GaussView, Version 5.0.9, Semichem Inc., Shawnee Mission, KS, 2009.

Conclusions

Tetra-porphyrin tweezer **2** with two remote but interdependent binding sites was synthesised *via* a divergent approach from a tetra-functional phenyl diimide core. The key step in obtaining this target was the application of a copper(II)-mediated coupling of benzene-1,4-diboronic acid with a polycyclic imide, and represents a novel use of such coupling in polycyclic scaffolds. We expect that the polycyclic imide coupling methodology presented in this paper, either *via* the phenyl boronic acid (superior for the synthesis of compound **10**) and/or aryl halide route, is easily and widely applicable to other modular polycyclic systems. This will aid in the synthesis of functional supramolecular architectures where control of north/south reactivity or other directional interactions is required. Furthermore, the microwave-accelerated ACE reaction allowed simultaneous attachment of the four porphyrin moieties to afford the tetra-porphyrin tweezer **2**.

Molecular modelling of both the equilibrium geometry of tetra-porphyrin tweezer **2** and the rotational energy profile of a model of the phenyl–imide linker core suggests the architecture is well suited for the complexation of diamino ligands of varying lengths, such as DABCO and 4,4′-bipy. This appears to be facilitated by bond rotation about both the central phenyl diimide core and the porphyrin receptors.

The absence of reactivity at the anhydride of laterally functionalised systems such as compound **4** continues to complicate efforts towards the convergent synthesis of extended polycyclic architectures. Our laboratory is currently pursuing the imide analogue of bis-porphyrin anhydride **7**, which is expected to be able to be coupled using the boronic acid method employed for the synthesis of compound **10**. The establishment of a convergent strategy would enable architecture **2** to be expanded to include asymmetric molecular tweezers with two different receptor binding sites.

Experimental

Molecular modelling

Molecular modelling was undertaken using the Wavefunction Spartan '10 software package.[79] Equilibrium geometry was calculated using a semi-empirical AM1 model. Rotational energy profiles were calculated using a Hartree–Fock 6-31G* model for each conformation about the bond specified by the dihedral angle constraint, with the energy of each conformation recalculated using a B3LYP/6-31G* Density Functional model to improve the fitting function.

Characterisation

Melting points were measured using a Barloworld Scientific SMP10 melting point apparatus.

NMR spectra were recorded on a Bruker UltraShield Avance III 400 MHz or 600 MHz NMR Spectrometer running the TopSpin software package at 299 K and 293 K respectively. Spectra were calibrated to the residual solvent signal.[83] $CDCl_3$ was deacidified by passing through neutral activated aluminium oxide (Scharlau, activity degree 1, 70–290 mesh, grain size 0.05–0.2 mm) and stored under a nitrogen atmosphere over silver foil/molecular sieves in a brown glass bottle.

Theoretical mass spectra were generated by using the mMass software package.[84]

Single crystals of compounds **11–13** suitable for X-ray diffraction experiments were covered in Paratone-N oil and mounted on a glass fibre. Data ($2\theta_{max}$ 55°) were collected at 150 K using an Oxford Diffraction X-Calibur X-ray diffractometer and MoK_α (λ 0.71073 Å) radiation. After integration and scaling, the datasets were merged into N unique reflections (R_{int}). The structures were solved using conventional methods and refined by using full-matrix least-squares using the SHELX-97 software[85] in conjunction with the X-Seed interface.[86] Non-hydrogen atoms were refined with anisotropic thermal parameters and hydrogen atoms were placed in calculated positions. Early refinement of compound **13** in an alternate monoclinic space group ($P2_1/n$) was attempted; however, structural solution in this space group failed. The structure was solved and refined in the more orthogonal space group $P2_1/c$. Structure solution and refinement succeeded with three crystallographically independent but structurally identical molecules in the asymmetric unit. Intensity data for compound **9** was collected with an Oxford Diffraction SuperNova CCD diffractometer using Cu-Kα radiation. The temperature during data collection was maintained at 100.0(1) using an Oxford Cryosystems cooling device. The structure was solved by direct methods and difference Fourier synthesis.[85] Thermal ellipsoid plots were generated using the program ORTEP-3[87] integrated within the WINGX[88] suite of programs. Additional information on the crystal structures of compounds **9** and **11–13** can be found in the ESI (see S8 and S15†). CCDC 1486427–1486430 contain the supplementary crystallographic data for this paper.

Where necessary, solvents and reagents for synthesis were purified according to the methods published.[89] Dry THF was freshly distilled from sodium/benzophenone, dry CH_2Cl_2 freshly distilled from CaH_2, and dry DMF and DMSO were distilled under reduced pressure onto fresh molecular sieves after stirring on molecular sieves overnight. Potassium *tert*-butoxide was purified by sublimation under high vacuum at 0.17 mmHg at 160 °C, stored under a nitrogen atmosphere, protected from light, and in a desiccator at room temperature. Benzene-1,4-diboronic acid (Sigma-Aldrich) was recrystallised from THF/H_2O and dried *in vacuo* at 50 °C for 3 hours. Zinc dust was treated with 2% hydrochloric acid to remove zinc oxide. LiHMDS and 4-methoxybenzylamine are available from Sigma-Aldrich.

Silica gel (Davisil, 60 Å, 40–63 μm, Grace Davison Discovery Sciences) was used for column chromatography. Kieselgel silica gel 60 F254 aluminium sheets (Merck) was used for TLC. Colourless compounds were visualised using a UV lamp or permanganate dip stain.

General procedure for microwave-accelerated ACE reactions

Microwave reactions were performed in a CEM Discover S-Class microwave in 10 mL reaction vessels loaded with 0.25 g combined starting materials suspended in no more than 2–3 mL of dry THF. The ACE reaction conditions are based on those prescribed.[43] The microwave was operated in variable power (dynamic) mode with the following parameters: temperature 170–180 °C, power 300 W, stirring high, compressed air cooling (PowerMAX) off. Ramp time to reach temperature set point was approximately 10–30 minutes, with the pressure reaching between 8–16.5 bar (maximum pressure cut-off 20 bar). The sample was held at the set temperature for a further 1–2 hours, with the microwave input power automatically modulated between 80–220 W. The pressure tapered off during the course of the reaction.

Synthesis of compounds

Mitsudo anhydride 4 .[42] Using a similar method to the literature,[90] a solution of anhydride **3**[49] (1.0 g, 4.31 mmol), DMAD[91,92] (1.3 g, approx. 2 eq., 9.15 mmol), and $[RuH_2(CO)(PPh_3)_3]$[93] (0.2 g, 0.22 mmol, 5 mol%) in toluene (20 mL) was heated at 80 °C for 4 days under a nitrogen atmosphere and protected from light, forming a white precipitate. The mixture was cooled, filtered, and the precipitate washed with EtOAc to afford a white powder (1.92 g, 86%), used for subsequent synthesis without further purification. M.p. decomposition 272–276 °C. ^{1}H NMR (400 MHz, $CDCl_3$, 26 °C): 4.83 (s, 4H), 3.81 (s, 12H), 3.27 (s, 4H). ^{13}C NMR (100 MHz, $CDCl_3$): 166.69, 160.04, 140.00, 77.74, 72.87, 52.48, 44.57. HRMS (ESI-TOF-MS) for $C_{24}H_{20}O_{13}Na^+$ $[M + Na]^+$: Calc: 539.0802. Found: 539.0801.

Bis-epoxide anhydride 5. Mitsudo anhydride **4** (1.0 g, 1.94 mmol) was dissolved in dry CH_2Cl_2 (100 mL) under a nitrogen atmosphere and cooled to 0 °C. Anhydrous *tert*-butyl hydroperoxide in toluene[94] (3.3 M, 1.47 mL, 4.85 mmol, 2.5 eq.) was added and stirred for a further 10 min at 0 °C, after which sublimed potassium *tert*-butoxide (0.21 g, 1.87 mmol, ~1 eq.) was added. The mixture was allowed to warm to room temperature over 30 minutes, during which a white precipitate formed. After stirring at room temperature for a further 3 hours, sodium sulfite (10% aqueous solution, 10 mL) was added with vigorous stirring for 15 minutes. The mixture was diluted with $CHCl_3$ (100 mL), washed with brine (200 mL), HCl (2 M, 100 mL), NaOH (2 M, 100 mL), H_2O (100 mL), dried with Na_2SO_4, filtered, and the solvent removed *in vacuo* to afford an off-white powder (0.52 g, 49%). The material was purified by passage through a plug (silica, CH_2Cl_2), followed by column chromatography (silica, CH_2Cl_2 to remove impurity, followed by elution of product with THF). This afforded white and pale yellow flakes used for subsequent reactions. A sample was recrystallised from $CHCl_3$/toluene (white powder precipitates during rotatory evaporation to reduce volume) for MS and melting point analysis. M.p. (solvent of crystallisation loss 180–185 °C, then partial

decomposition), >300 °C. ^{1}H NMR (400 MHz, $CDCl_3$, 26 °C): 5.57 (s, 4H), 3.84 (s, 12H), 2.94 (s, 4H). ^{13}C NMR (150 MHz, $CDCl_3$): 165.98, 163.31, 80.84, 73.16, 62.68, 53.33, 48.57. HRMS (ESI-TOF-MS) for $C_{24}H_{20}O_{15}Na$ $[M + Na]^+$: Calc. 571.0700. Found. 571.0688.

Bis-porphyrin anhydride 7. A suspension of bis-epoxide anhydride **5** (50 mg, 0.09 mmol) and *exo*-imide porphyrin receptor **6** (166 mg, 0.21 mmol, ~2 eq.) in dry THF (3 mL) was subjected to microwave irradiation using the conditions in the ACE general procedure, forming a purple precipitate. The precipitate was filtered, and washed with THF, $CHCl_3$, CH_3CN, toluene, EtOAc, MeOH, and hexane to afford a purple solid (130 mg, 68%), which exhibited extremely poor solubility in many solvents ($CHCl_3$, CH_3CN, EtOAc, THF, acetone, DMSO, toluene, pyridine) with the exception of acids (TFA, H_2SO_4). No NMR or UV-Vis data were obtained (insoluble). M.p. >300 °C. HRMS (ESI-TOF-MS) for $C_{130}H_{96}N_{10}O_{19}^{2+}$ $[M + 2H]^{2+}$: Calc: 1050.3421. Found 1050.3432.

Non-Mitsudo phenyl diimide 9. Using an alternative method to that described,[44] *p*-phenylenediamine (0.188 g, 1.74 mmol) was dissolved in dry degassed THF (50 mL) under an argon atmosphere. LiHMDS[54] (900 μL, 0.9 mmol, ≪1 eq., 1 M in THF, Sigma-Aldrich) was added dropwise from a syringe with stirring over 10–15 seconds, giving a pale yellow solution. After 30 minutes, bis-acid chloride **8** [38,48] (1.0 g, 3.48 mmol, 2 eq.) was added in portions as a solid, immediately forming a precipitate. Although no change was observed after 1 hour, the mixture was allowed to stir overnight for good measure, the precipitate filtered and washed with Et_2O to afford a red/brown powder (0.46 g, 0.78 mmol, 86%, NMR consistent with amic acid). The powder was subjected to ring closing conditions[38] using the following procedure. The powder was suspended in dry THF (50 mL) under an argon atmosphere, and HOBt (at least 0.32 g, 2.33 mmol, at least 3 eq.) added with stirring. After 5 minutes, DCC (at least 0.48 g, 2.33 mmol, at least 3 eq.**) and Et_3N (1.1 mL, 7.8 mmol, ~10 eq.) were added in quick succession and the mixture stirred at room temperature for 4 days (ring closing halfway), then at 50 °C for a further 2 days. The mixture was cooled and filtered, and the solids washed with hexane (100 mL), acetone (100 mL), CH_3CN (100 mL), EtOH (100 mL), and hexane (100 mL) to remove impurity (product sparingly soluble). The remaining solid was dissolved in CH_2Cl_2 (200 mL) and washed with HCl (2 M, 100 mL) NaOH (2 M, 100 mL), H_2O (100 mL), dried with Na_2SO_4, filtered, and the solvent removed *in vacuo* to afford a beige powder. M.p. >300 °C. ^{1}H NMR (600 MHz, $CDCl_3$, 20 °C): 7.12 (s, 4H), 6.73 (s, 8H), 5.35 (s, 8H). ^{13}C NMR (150 MHz, $CDCl_3$): 172.91, 139.37, 131.28, 126.69, 81.73, 69.35. HRMS (ESI-TOF-MS) for $C_{30}H_{20}N_2O_8Na^+$ $[M + Na]^+$: Calc: 559.1117. Found: 559.1123. Single crystal grown from DMSO by slow evaporation for X-ray diffraction. CCDC 1486430 contains the supplementary crystallographic data for this paper.

PMB protected imide 11. Using modified procedure,[18,50] anhydride **3** [49] (21 g, 0.090 mol) was dissolved in $CHCl_3$ (300 mL, deacidified by passing through neutral activated aluminium oxide) under a nitrogen atmosphere. 4-Methoxybenzylamine (2 eq., 25 g per 23.6 mL, 0.18 mol, Sigma-Aldrich) was added and the solution stirred at 50 °C overnight under a nitrogen atmosphere, during which a white precipitate formed. The mixture was cooled, filtered, and the precipitate washed with $CHCl_3$ (3 × 100 mL). The precipitate was dissolved in Ac_2O (350 mL), NaOAc (2 eq., 24.6 g, 0.181 mol) added, and the mixture stirred overnight at 50 °C under a nitrogen atmosphere, after which the Ac_2O was removed by distillation under reduced pressure at 50 °C. The solids were redissolved into $CHCl_3$ (300 mL), washed with H_2O (2 × 200 mL), HCl (2 M, 200 mL), NaOH†† (2 M, 5 × 200 mL), H_2O (200 mL), dried with Na_2SO_4, filtered, and the solvent removed *in vacuo*. The solid was washed with hexane (2 × 100 mL), Et_2O (2 × 100 mL), and EtOH (5 × 100 mL, to remove significant brown byproduct) to afford a white powder (16.5 g, 52%). A sample was recrystallised from $CHCl_3$/hexane for MS and melting point analysis. M.p. 231–233 °C. ^{1}H NMR (600 MHz, $CDCl_3$, 20 °C): 7.15 (d, J = 8.8 Hz, 2H), 6.79 (d, 8.8 Hz, 2H), 6.37 (m, 4H), 5.20 (m, 4H), 4.28 (s, 2H), 3.77 (s, 3H). ^{13}C NMR (150 MHz, $CDCl_3$): 173.86, 159.31, 138.90, 130.51, 127.28, 113.74, 81.39, 69.21, 55.30, 41.79. HRMS (ESI-TOF-MS) for $C_{20}H_{17}NO_5Na^+$ $[M + Na]^+$: Calc: 374.1004. Found: 374.1000. Single crystals for X-ray analysis were grown from CH_3CN by slow evaporation. CCDC 1486427 contains the supplementary crystallographic data for this paper.

Imide 12. Using a modified procedure,[18,50–53] PMB protected imide **11** (16 g, 0.046 mol) was slowly dissolved in a mixture of 9 : 1 CH_3CN/H_2O (1 L) at 40 °C for 1 h. Ammonium cerium(IV) nitrate (82 g, 3.3 eq.) was added in two portions; 2.3 eq. for 90 min, followed by 1 eq. for a further 30 minutes; with reaction progress monitored by NMR. The volume of the solution was reduced by approximately two thirds *in vacuo* at 50 °C, or until a precipitate formed. The precipitate was filtered and put aside to later be combined with additional product. The filtrate volume was then further reduced *in vacuo* at 50 °C until only H_2O remained. The mixture was diluted with further H_2O, extracted with EtOAc (10 × 200 mL), and the EtOAc extracts combined. The volume of EtOAc was reduced *in vacuo* at 50 °C until a precipitate formed. The precipitate was filtered, and combined with the first crop of product. The filtrate volume was further reduced, and the precipitate collection cycle repeated until only an orange/brown oily sludge remained (*p*-anisaldehyde byproduct). The combined precipitate was washed with H_2O (2 × 100 mL) and EtOH (10 × 100 mL) to afford a white powder (7.64 g, 73%). M.p. partial decomposition (darkens) >200 °C, violent decomposition (boiling) at 293–295 °C. Single crystals for X-ray analysis were grown from CH_3CN/DMSO by slow evaporation. ^{1}H NMR (600 MHz,

** An excess of warm DCC was added as a liquid.

†† **Caution**: NaOH reacts exothermically with residual Ac_2O, temperature should remain below 50 °C for optimum product stability.

DMSO-d_6, 20 °C): 10.79 (s, 1H), 6.71 (s, 4H), 5.24 (s, 4H). ^{13}C NMR (150 MHz, DMSO-d_6): 175.34, 139.36, 80.39, 70.03. HRMS (ESI-TOF-MS) for $C_{12}H_8NO_4^-$ $[M - H]^-$: Calc: 230.0453. Found: 230.0457. CCDC 1486428 contains the supplementary crystallographic data for this paper.

Mitsudo imide 13. A solution of imide **12** (5.0 g, 0.022 mol), DMAD[91,92] (12.3 g, 0.087 mol, 4 eq.), and $[RuH_2(CO)(PPh_3)_3]$[93] (7.2 g, 2.4 mmol, 36 mol%) in dry DMF (150 mL) was stirred at 60 °C under a nitrogen atmosphere for 1 day. The black solution was cooled, and the DMF removed by distillation under reduced pressure. The remaining sludge was purified by several rounds of column chromatography using different solvents to elute the product as follows: (1) (silica, plug, 20% THF/$CHCl_3$), collecting several large plug length fractions, NMR to determine fractions which contained product, (2) these fractions recolumned (silica, 5% THF/$CHCl_3$), collecting the middle band, (3) and this fraction recolumned (silica, EtOAc). The solvent was removed *in vacuo*, and the product recrystallised from EtOAc/hexane or $CHCl_3$/hexane to afford a white to pale yellow powder (3.81 g, 34%). M.p. (solvent of crystallisation loss 282–302 °C), 303–307 °C (decomposition). Single crystals for X-ray analysis were grown from CH_3CN by slow evaporation. ^{1}H NMR (600 MHz, $CDCl_3$, 20 °C): 7.80 (s, 1H), 4.75 (s, 4H), 3.79 (s, 12H), 3.24 (s, 4H). ^{13}C NMR (150 MHz, $CDCl_3$): 172.12, 160.25, 140.19, 77.11, 71.57, 52.43, 44.82. HRMS (ESI-TOF-MS) for $C_{24}H_{20}NO_{12}^-$ $[M - H]^-$: Calc: 514.0986. Found: 514.0982. CCDC 1486429 contains the supplementary crystallographic data for this paper.

Mitsudo phenyl imide 14a

Method A – microwave/aryl halide/Cu(0). Using a modified procedure (*N*-aryl imides from succinimide/phthalimide and mono-halo aryl[57]), Mitsudo imide **13** (100 mg, 0.19 mmol), activated elemental copper[95] ‡‡ (100 mg, 1.57 mmol, at least 5 eq.), and iodobenzene (500 μL, 0.44 mmol, solvent/excess) were suspended in a 10 mL microwave vessel. The microwave was operated in variable power (dynamic) mode with the following parameters: temperature 150 °C, power 300 W (automatically modulated around the set temperature), stirring high, compressed air cooling (PowerMAX) on. The sample was held at this temperature 10 minutes, and this repeated for 3–4 cycles, removing the sample in between runs to check the vessel integrity, ensure thorough mixing, and was recharged with additional iodobenzene (500 μL) as necessary if the contents had thickened to a paste or solidified. The mixture was diluted with EtOAc (100 mL), filtered to remove Cu(0), and any solids washed with $CHCl_3$ (100 mL). The combined EtOAc/$CHCl_3$ solution was washed with KOH (2 M, 2 × 100 mL), H_2O (2 × 100 mL), dried with Na_2SO_4, and the solvents removed *in vacuo*. The residual iodobenzene was diluted with hexane to precipitate the product, which was filtered and washed with hexane to afford a white powder. ^{1}H NMR (600 MHz, $CDCl_3$, 20 °C): 7.53–7.48 (m, 2H), 7.48–7.44 (m, 1H), 7.20–7.16 (m, 2H), 4.87 (s, 4H), 3.80 (s, 12H), 3.28 (s, 4H). HRMS (ESI-TOF-MS) for $C_{30}H_{25}NO_{12}Na^+$ $[M + Na]^+$: Calc. 614.1274. Found. 614.1279.

Method B – phenyl boronic acid/Cu(II)/air. Using the method developed from ref. 59 and used for Mitsudo phenyl diimide **10** (described later), the reaction was undertaken on Mitsudo imide **13** using phenyl boronic acid. The crude sample mixture contained the same ^{1}H NMR resonances assigned to product from Method A.

Mitsudo 4-iodophenyl imide 14b. Using a modified procedure,[57] Mitsudo imide **13** (100 mg, 0.19 mmol), activated elemental copper[59]†† (100 mg, 1.57 mmol), and 1,4-diiodobenzene (500 mg, 1.52 mmol, excess) were suspended in solvent (EtOAc, 1 mL) in a 10 mL microwave vessel. The microwave was operated in variable power (dynamic) mode with the following parameters: temperature 120–150 °C, power 300 W (automatically modulated around the set temperature), stirring high, compressed air cooling (PowerMAX) on. The mixture was microwaved at 120 °C for 1 h, further activated copper (100 mg, 1.57 mmol) added, and microwaved for an additional 1.5 h (total 2.5 h). The mixture was charged with toluene (1 mL), and microwaved at 150 °C for an additional 1 h (total 3.5 h), during which temperature and pressure stability seemed to be restored. NMR after 3.5 h total reaction time indicated just 30% conversion to the coupled adduct. The mixture was microwaved for a total of 12 h, after which NMR indicated approximately 66% conversion to the coupled adduct. The yellow/brown liquid was filtered, the solids washed with toluene (50 mL), EtOAc (50 mL), $CHCl_3$ (50 mL), the solvent removed *in vacuo*, and purified by column chromatography (silica, 20% EtOAc/$CHCl_3$) to afford a white powder (20 mg, 14%). ^{1}H NMR (600 MHz, $CDCl_3$, 20 °C): 7.83 (d, 2H, J = 8.61 Hz), 6.95 (d, 2H, J = 8.61 Hz), 4.86 (s, 4H), 3.79 (s, 12H), 3.22 (s, 4H). HRMS (ESI-TOF-MS) for $C_{30}H_{24}NO_{12}INa^+$ $[M + Na]^+$: Calc. 740.0241. Found. 740.0251.

Mitsudo phenyl diimide 10. Using a modified procedure developed for coupling nitrogen-containing compounds with aryl mono-boronic acid derivatives,[58,59] Mitsudo imide **13** (380 mg, 0.74 mmol) was suspended in MeOH (25 mL), and compressed air bubbled through a large gauge needle into the reaction mixture at a flow rate of 3–4 bubbles per second. Benzene-1,4-diboronic acid (61 mg, 0.37 mmol, Sigma-Aldrich) was added, quickly followed by $Cu(OAc)_2{\cdot}H_2O$ (7.5 mg, 0.038 mmol, no more than 2.5–5 mol% per boronic acid). The mixture was refluxed for 12 hours during which a white precipitate formed. The volume of MeOH was monitored for evaporation and maintained. The air bubbler needle was changed every 1 hour to prevent clogging, while the air flow rate was varied as necessary to maintain the blue/green colour of the solution (greater air flow required if the solution was brown), yet without cooling the mixture and preventing reflux. The reaction produced two compounds, the Mitsudo phenyl diimide **10** (precipitate), and a solvent-dependent side product (filtrate). The side product in the filtrate (**15a**, **15b**) was

‡‡ Prior to precipitation of copper, the zinc dust was pre-treated with 2% hydrochloric acid to ensure it met the oxide-free requirement. Freshly precipitated elemental copper was dried *in vacuo*, and not at 100 °C. The elemental copper appeared as more of a brown powder (not metallic/lustrous in appearance).

characterised without further purification. The desired product (precipitate) was purified using the following method:

The mixture was cooled, the precipitate removed by filtration, and the solids washed with MeOH (100 mL). The solid was dissolved in CH_2Cl_2 (100 mL), washed with H_2O (100 mL), dried with Na_2SO_4, the solvent removed *in vacuo*, and washed again with MeOH (100 mL) and hexane (100 mL) to afford a white powder (150 mg, 37%). This procedure was repeated several times on a similar scale to generate additional material. A sample was recrystallised from $CHCl_3$/hexane for MS and melting point analysis. M.p. >300 °C (partial decomposition). ^{1}H NMR (600 MHz, $CDCl_3$, 20 °C): 7.38 (s, 4H), 4.87 (s, 8H), 3.80 (s, 24H), 3.23 (s, 8H). ^{13}C NMR (150 MHz, $CDCl_3$): 171.50, 160.17, 140.11, 131.21, 127.03, 77.61, 70.37, 52.49, 44.82. HRMS (ESI-TOF-MS) for $C_{54}H_{44}N_2O_{24}Na^+$ $[M + Na]^+$: Calc: 1127.2182. Found: 1127.2166.

Side product with solvent MeOH, ***15a****.* ^{1}H NMR (600 MHz, $CDCl_3$, 20 °C): 7.08 (d, 2H, J = 9.0 Hz), 6.99 (d, 2H, J = 9.0 Hz), 4.86 (s, 4H), 3.84 (s, 3H), 3.80 (s, 12H), 3.26 (s, 4H). HRMS (ESI-TOF-MS) for $C_{31}H_{27}NO_{13}Na^+$ $[M + Na]^+$: Calc. 644.1380. Found. 644.1362.

Side product with solvent 9 : 1 THF/H_2O, ***15b****.* ^{1}H NMR (600 MHz, $CDCl_3$, 20 °C): 7.04 (d, 2H, J = 8.9 Hz), 6.93 (d, 2H, J = 8.9 Hz), 5.31 (s, 1H), 4.86 (s, 4H), 3.80 (s, 12H), 3.25 (s, 4H). HRMS (ESI-TOF-MS) for $C_{30}H_{25}NO_{13}Na^+$ $[M + Na]^+$: Calc. 630.1224. Found. 630.1203.

Tetra-epoxide phenyl diimide linker 16. Mitsudo phenyl diimide **10** (300 mg, 0.27 mmol) was dissolved in dry CH_2Cl_2 (100 mL) under a nitrogen atmosphere and cooled to 0 °C. Anhydrous *tert*-butyl hydroperoxide in toluene[94] (3.3 M, 0.55 mL, 1.82 mmol, at least 5 eq.) was added and stirred for a further 10 min at 0 °C, after which sublimed potassium *tert*-butoxide (70 mg, 0.62 mol, approx. 2 eq.) was added. The mixture was allowed to warm to room temperature over 30 minutes, and after stirring at room temperature for a further 3 hours, the mixture was diluted with CH_2Cl_2 (50 mL) and sodium sulfite (10% aqueous solution, 10 mL) added with vigorous stirring for 15 minutes. The mixture was further diluted with CH_2Cl_2 (200 mL), washed with brine (200 mL), dried with Na_2SO_4, filtered, and the solvent removed *in vacuo*. This afforded a white powder (160 mg, 50%), used in subsequent reactions without further purification. A sample was recrystallised from CH_2Cl_2/hexane for MS and melting point analysis. M.p. >300 °C (partial decomposition 200 °C). ^{1}H NMR (600 MHz, CD_2Cl_2, 20 °C): 7.26 (s, 4H), 5.60 (s, 8H), 3.81 (s, 24H), 2.87 (s, 8H). ^{13}C NMR (150 MHz, CD_2Cl_2): 171.30, 163.63, 131.30, 127.36, 80.95, 70.86, 63.03, 53.35, 49.15. HRMS (ESI-TOF-MS) for $C_{54}H_{44}N_2O_{28}Na^+$ $[M + Na]^+$: Calc: 1191.1978. Found (two different samples): 1191.1984, 1191.2006.

Free base tetra-porphyrin tweezer 2. A suspension of quad-epoxide phenyl diimide linker **16** (55 mg, 0.047 mmol) and *exo*-imide porphyrin receptor **6** (180 mg, 0.23 mmol, 4.9 eq.) in dry THF (3 mL) was subjected to microwave irradiation using the conditions in the general procedure at the beginning of the experimental. This procedure was repeated several times on a similar scale until 150 mg (0.128 mmol) epoxide had been reacted. The material from each reaction was combined, the solvent removed *in vacuo*, and the material purified by column chromatography (silica, $CHCl_3$) to recover unreacted *exo*-imide porphyrin receptor **6**, after which the mobile phase was changed to 10% THF/$CHCl_3$ and the strong porphyrin band collected. ^{1}H NMR of this material suggested the band contained a majority of the desired tetra-porphyrin adduct with small amounts of other porphyrin stoichiometries. The material was recrystallised twice from $CHCl_3$/MeOH to afford purple crystals of the pure tetra-porphyrin tweezer (88 mg, 16%). ^{1}H NMR (600 MHz, $CDCl_3$, 20 °C, approximately 0.8 mM): 8.83 (s, 32H), 8.30 (bs, 8H), 8.23–8.13 (m, 24H), 7.80 (s, 4H), 7.79–7.69 (m, 36H), 7.65 (bs, 8H), 4.94 (s, 8H), 4.02 (s, 24H), 2.96 (bs, 8H), 2.91 (s, 8H), 2.67 (s, 8H), 2.63 (d, 11.67 Hz, 4H), 2.36 (s, 8H), 1.28 (d, 11.67 Hz, 4H), −2.81 (s, 8H). HRMS (ESI-TOF-MS) for: $C_{266}H_{196}N_{22}O_{36}{}^{4+}$ $[M + 4H]^{4+}$: Calc: 1068.3540. Found 1068.3566. $C_{266}H_{195}N_{22}O_{36}{}^{3+}$ $[M + 3H]^{3+}$: Calc: 1424.1363. Found 1424.1392. $C_{266}H_{194}N_{22}O_{36}{}^{2+}$ $[M + 2H]^{2+}$: Calc: 2135.7008. Found 2135.7022. UV-Vis ($CHCl_3$): λ_{max} (nm) = 419.0 (shoulder around 400), 515.2, 550.8, 590.0, 644.6.

Acknowledgements

R. B. M. thanks Flinders University for the provision of an Australian Postgraduate Award and the Playford Memorial Trust for a PhD top-up scholarship. R. B. M. also thanks Dr Sally Duck (Monash University) for efforts and expertise in accurate mass spectrometry determination of the porphyrin compounds **2** and **7**.

Notes and references

1 J. Rebek Jr., J. E. Trend, R. V. Wattley and S. Chakravorti, *J. Am. Chem. Soc.*, 1979, **101**, 4333–4337.
2 J. Rebek Jr. and R. V. Wattley, *J. Am. Chem. Soc.*, 1980, **102**, 4853–4854.
3 J. Rebek Jr. and L. Marshall, *J. Am. Chem. Soc.*, 1983, **105**, 6668–6670.
4 Y. Kubo, Y. Murai, J.-i. Yamanaka, S. Tokita and Y. Ishimaru, *Tetrahedron Lett.*, 1999, **40**, 6019–6023.
5 Y. Kubo, T. Ohno, J.-i. Yamanaka, S. Tokita, T. Iida and Y. Ishimaru, *J. Am. Chem. Soc.*, 2001, **123**, 12700–12701.
6 M. Ayabe, A. Ikeda, S. Shinkai, S. Sakamoto and K. Yamaguchi, *Chem. Commun.*, 2002, 1032–1033.
7 C.-H. Lee, H. Yoon and W.-D. Jang, *Chem. – Eur. J.*, 2009, **15**, 9972–9976.
8 J. Leblond, H. Gao, A. Petitjean and J.-C. Leroux, *J. Am. Chem. Soc.*, 2010, **132**, 8544–8545.
9 H. Sato, K. Tashiro, H. Shinmori, A. Osuka, Y. Murata, K. Komatsu and T. Aida, *J. Am. Chem. Soc.*, 2005, **127**, 13086–13087.
10 H. Sato, K. Tashiro, H. Shinmori, A. Osuka and T. Aida, *Chem. Commun.*, 2005, 2324–2326.

11 R. B. Murphy, D.-T. Pham, S. F. Lincoln and M. R. Johnston, *Eur. J. Org. Chem.*, 2013, 2985–2993.
12 R. N. Warrener, D. N. Butler, W. Y. Liao, I. G. Pitt and R. A. Russell, *Tetrahedron Lett.*, 1991, **32**, 1889–1892.
13 R. N. Warrener, I. G. Pitt and D. N. Butler, *J. Chem. Soc., Chem. Commun.*, 1983, 1340–1342.
14 R. N. Warrener, A. C. Schultz, D. N. Butler, S. Wang, I. B. Mahadevan and R. A. Russel, *Chem. Commun.*, 1997, 1023–1024.
15 R. N. Warrener, S. Wang and R. A. Russell, *Tetrahedron*, 1997, **53**, 3975–3990.
16 R. N. Warrener, D. N. Butler, D. Margetic, F. M. Pfeffer and R. A. Russell, *Tetrahedron Lett.*, 2000, **41**, 4671–4675.
17 A. M. Napper, I. Read, N. J. Head, A. M. Oliver and M. N. Paddon-Row, *J. Am. Chem. Soc.*, 2000, **122**, 5220–5221.
18 N. J. Head, A. M. Oliver, K. Look, N. R. Lokan, G. A. Jones and M. N. Paddon-Row, *Angew. Chem., Int. Ed.*, 1999, **38**, 3219–3222.
19 M. J. Shephard and M. N. Paddon-Row, *J. Phys. Chem. A*, 2000, **104**, 11628–11635.
20 M. J. Shephard and M. N. Paddon-Row, *J. Phys. Chem. A*, 1999, **103**, 3347–3350.
21 M. R. Johnston and D. M. Lyons, *Supramol. Chem.*, 2005, **17**, 503–511.
22 M. R. Johnston, M. J. Latter and R. N. Warrener, *Org. Lett.*, 2002, **4**, 2165–2168.
23 M. D. Johnstone, E. K. Schwarze, J. Ahrens, D. Schwarzer, J. J. Holstein, B. Dittrich, F. M. Pfeffer and G. H. Clever, *Chem. – Eur. J.*, 2016, **22**, 10791–10795.
24 M. D. Johnstone, M. Frank, G. H. Clever and F. M. Pfeffer, *Eur. J. Org. Chem.*, 2013, 5848–5853.
25 M. Shang, R. N. Warrener, D. N. Butler, Y. Murata and D. Margetić, *Mol. Diversity*, 2011, **15**, 541–560.
26 P. Trošelj, A. Briš, Y. Murata and D. Margetić, *Struct. Chem.*, 2012, **23**, 791–799.
27 P. Trošelj, I. Đilović, D. Matković-Čalogović and D. Margetić, *J. Heterocycl. Chem.*, 2013, **50**, 83–90.
28 M. Golić, M. R. Johnston, D. Margetić, A. C. Schultz and R. N. Warrener, *Aust. J. Chem.*, 2006, **59**, 899–914.
29 D. Margetic, M. R. Johnston, E. R. T. Tiekink and R. N. Warrener, *Tetrahedron Lett.*, 1998, **39**, 5277–5280.
30 M. Johnston, *Molecules*, 2001, **6**, 406–416.
31 D. Margetic, R. N. Warrener, D. N. Butler and D. Officer, *Theor. Chem. Acc.*, 2007, **117**, 239–245.
32 J. M. Lawson, A. M. Oliver, D. F. Rothenfluh, Y.-Z. An, G. A. Ellis, M. G. Ranasinghe, S. I. Khan, A. G. Franz, P. S. Ganapathi, M. J. Shephard, M. N. Paddon-Row and Y. Rubin, *J. Org. Chem.*, 1996, **61**, 5032–5054.
33 T. D. M. Bell, K. A. Jolliffe, K. P. Ghiggino, A. M. Oliver, M. J. Shephard, S. J. Langford and M. N. Paddon-Row, *J. Am. Chem. Soc.*, 2000, **122**, 10661–10666.
34 R. N. Warrener, D. N. Butler, L. Liu, D. Margetic and R. A. Russell, *Chem. – Eur. J.*, 2001, **7**, 3406–3414.
35 M. J. Gunter, H. Tang and R. N. Warrener, *J. Porphyrins Phthalocyanines*, 2002, **6**, 673–684.
36 M. R. Johnston, M. J. Latter and R. N. Warrener, *Aust. J. Chem.*, 2001, **54**, 633–636.
37 H. Tang, Z. Dong, Z. Merican, D. Margetić, Ž. Marinić, M. J. Gunter, D. Officer, D. N. Butler and R. N. Warrener, *Tetrahedron Lett.*, 2009, **50**, 667–670.
38 S. P. Gaynor, M. J. Gunter, M. R. Johnston and R. N. Warrener, *Org. Biomol. Chem.*, 2006, **4**, 2253–2266.
39 G. Ercolani and L. Schiaffino, *Angew. Chem., Int. Ed.*, 2011, **50**, 1762–1768.
40 T.-a. Mitsudo, K. Kokuryo, T. Shinsugi, Y. Nakagawa, Y. Watanabe and Y. Takegami, *J. Org. Chem.*, 1979, **44**, 4492–4496.
41 T.-a. Mitsudo, H. Naruse, T. Kondo, Y. Ozaki and Y. Watanabe, *Angew. Chem., Int. Ed. Engl.*, 1994, **33**, 580–581.
42 G. Dennison, unpublished work, 2004.
43 R. C. Foitzik, A. Lowe and F. M. Pfeffer, *Tetrahedron Lett.*, 2009, **50**, 2583–2584.
44 S. Gaynor, PhD thesis, University of New England, Armidale, New South Wales, 2003.
45 T.-C. Chou, K.-C. Lin and C.-A. Wu, *Tetrahedron*, 2009, **65**, 10243–10257.
46 O. Diels and K. Alder, *Justus Liebigs Ann. Chem.*, 1931, **490**, 243–257.
47 J. Kallos and P. Deslongchamps, *Can. J. Chem.*, 1966, **44**, 1239–1245.
48 G. Maier and W. A. Jung, *Chem. Ber.*, 1982, **115**, 804–807.
49 D. Margetic, R. N. Warrener, G. Sun and D. N. Butler, *Tetrahedron*, 2007, **63**, 4338–4346.
50 D. Mink and G. Deslongchamps, *Tetrahedron Lett.*, 1996, **37**, 7035–7038.
51 M. Yamaura, T. Suzuki, H. Hashimoto, J. Yoshimura and T. Okamoto, *Bull. Chem. Soc. Jpn.*, 1985, **58**, 1413–1420.
52 J. Yoshimura, M. Yamaura, T. Suzuki and H. Hashimoto, *Chem. Lett.*, 1983, 1001–1002.
53 D. G. Lonergan, PhD, The University of New Brunswick, 1998.
54 L. Barriault and P. A. Evans, Personal Communication while visiting Flinders University, 2011.
55 R. B. Murphy, PhD thesis, Flinders University, Adelaide, South Australia, 2016.
56 R. N. Warrener, D. Margetic, A. S. Amarasekara, D. N. Butler, I. B. Mahadevan and R. A. Russell, *Org. Lett.*, 1999, **1**, 199–202.
57 L. D. S. Yadav, B. S. Yadav and V. K. Rai, *Synthesis*, 2006, 1868–1872.
58 J.-B. Lan, G.-L. Zhang, X.-Q. Yu, J.-S. You, L. Chen, M. Yan and R.-G. Xie, *Synlett*, 2004, 1095–1097.
59 J.-B. Lan, L. Chen, X.-Q. Yu, J.-S. You and R.-G. Xie, *Chem. Commun.*, 2004, 188–189.
60 C. W. Miller, C. E. Hoyle, E. J. Valente, D. H. Magers and E. S. Jönsson, *J. Phys. Chem. A*, 1999, **103**, 6406–6412.
61 C. W. Miller, E. S. Jönsson, C. E. Hoyle, K. Viswanathan and E. J. Valente, *J. Phys. Chem. B*, 2001, **105**, 2707–2717.
62 C. Miller, C. Hoyle, E. Valente, J. Zubkowski and E. S. Jönsson, *J. Chem. Crystallogr.*, 2000, **30**, 563–571.
63 B. A. Langowski, R. Rothchild and A.-M. Sapse, *Spectrosc. Lett.*, 2001, **34**, 235–251.

64 K. Kondo, H. Fujita, T. Suzuki and Y. Murakami, *Tetrahedron Lett.*, 1999, **40**, 5577–5580.
65 M. Mao, J. England and S. R. Turner, *Polymer*, 2011, **52**, 4498–4502.
66 Y. Yu, L. Shi, D. Yang and L. Gan, *Chem. Sci.*, 2013, **4**, 814–818.
67 S. Verma and N. Singh, *Aust. J. Chem.*, 1976, **29**, 295–300.
68 D. P. Curran, S. Geib and N. DeMello, *Tetrahedron*, 1999, **55**, 5681–5704.
69 K. Tanaka, M. Okano, H. Toshino, H. Kita and K.-I. Okamoto, *J. Polym. Sci., Part B: Polym. Phys.*, 1992, **30**, 907–914.
70 Y. Zhang, J. M. Lavin and K. D. Shimizu, *J. Am. Chem. Soc.*, 2009, **131**, 12062–12063.
71 D.-S. Choi, Y. S. Chong, D. Whitehead and K. D. Shimizu, *Org. Lett.*, 2001, **3**, 3757–3760.
72 Y. Chen, M. D. Smith and K. D. Shimizu, *Tetrahedron Lett.*, 2001, **42**, 7185–7187.
73 R. D. Rasberry, X. Wu, B. N. Bullock, M. D. Smith and K. D. Shimizu, *Org. Lett.*, 2009, **11**, 2599–2602.
74 C. F. Degenhardt, J. M. Lavin, M. D. Smith and K. D. Shimizu, *Org. Lett.*, 2005, **7**, 4079–4081.
75 J. M. Lavin and K. D. Shimizu, *Chem. Commun.*, 2007, 228–230.
76 W. R. Carroll, P. Pellechia and K. D. Shimizu, *Org. Lett.*, 2008, **10**, 3547–3550.
77 D. P. Curran and N. C. DeMello, *J. Chem. Soc., Chem. Commun.*, 1993, 1314–1317.
78 A. M. Napper, N. J. Head, A. M. Oliver, M. J. Shephard, M. N. Paddon-Row, I. Read and D. H. Waldeck, *J. Am. Chem. Soc.*, 2002, **124**, 10171–10181.
79 Spartan '10 for Windows, Wavefunction, Inc., 18401 Von Karman Avenue, Suite 370, Irvine, CA 92612, USA, http://www.wavefun.com/index.html.
80 S. S. Eaton and G. R. Eaton, *J. Chem. Soc., Chem. Commun.*, 1974, 576–577.
81 R. W. Wagner, T. E. Johnson and J. S. Lindsey, *J. Am. Chem. Soc.*, 1996, **118**, 11166–11180.
82 S. S. Eaton and G. R. Eaton, *J. Am. Chem. Soc.*, 1975, **97**, 3660–3666.
83 H. E. Gottlieb, V. Kotlyar and A. Nudelman, *J. Org. Chem.*, 1997, **62**, 7512–7515.
84 mMass 5.4.1, Martin Strohalm, http://www.mmass.org/, 2012.
85 G. Sheldrick, *Acta Crystallogr., Sect. A: Fundam. Crystallogr.*, 2008, **64**, 112–122.
86 L. J. Barbour, *J. Supramol. Chem.*, 2001, **1**, 189–191.
87 L. Farrugia, *J. Appl. Crystallogr.*, 1997, **30**, 565.
88 L. Farrugia, *J. Appl. Crystallogr.*, 1999, **32**, 837–838.
89 D. D. Perrin, L. Armarego and D. R. Perrin, *Purification of Laboratory Chemicals*, Pergamon Press, Ltd, Oxford, 1966.
90 M. R. Johnston, personal communication.
91 E. H. Huntress, T. E. Lesslie and J. Bornstein, *Org. Syn. Coll.*, 1952, **32**, 55.
92 E. H. Huntress, T. E. Lesslie and J. Bornstein, *Org. Syn. Coll.*, 1963, **4**, 329.
93 S. D. Robinson, *Inorg. Synth.*, 1974, **15**, 48–50.
94 J. G. Hill, B. E. Rossiter and K. B. Sharpless, *J. Org. Chem.*, 1983, **48**, 3607–3608.
95 P. H. Gore and G. K. Hughes, *J. Chem. Soc.*, 1959, 1615–1616.